JOURNAL OF GEOPHYSICAL RESEARCH, VOL. 114, A12313, doi:10.1029/2009JA014568, 2009

Observations of the ionospheric response to the 15 December 2006 geomagnetic storm: Long-duration positive storm effect

N. M. Pedatella,[1] J. Lei,[1] K. M. Larson,[1] and J. M. Forbes[1]

Received 15 June 2009; revised 29 July 2009; accepted 21 August 2009; published 22 December 2009.

[1] The long-duration positive ionospheric storm effect that occurred on 15 December 2006 is investigated using a combination of ground-based Global Positioning System (GPS) total electron content (TEC), TOPEX and Jason-1 TEC, and topside ionosphere/plasmasphere TEC, GPS radio occultation, and tiny ionospheric photometer (TIP) observations from the Constellation Observing System for Meteorology, Ionosphere, and Climate (COSMIC) satellites. This multi-instrument approach provides a unique view of the ionospheric positive storm effect by revealing the storm time response in different altitude regions. The ground-based GPS TEC, TOPEX/Jason-1 TEC, and topside ionosphere/plasmasphere TEC all reveal significant enhancements at low latitudes to midlatitudes over the Pacific Ocean region during the initial portions of the storm main phase from 0000–0400 universal time (UT) on 15 December. At low latitudes, the topside ionosphere/plasmasphere TEC increase represents greater than 50% of the TEC enhancement that is observed by ground-based GPS receivers. Moreover, electron density profiles obtained using the technique of GPS radio occultation demonstrate that the F layer peak height increased by greater than 100 km during this time period. The effects of soft particle precipitation are also apparent in the COSMIC observations of topside ionosphere/plasmasphere TEC. The positive storm effects over the Pacific Ocean region remain present in the equatorial ionization anomaly crest regions beyond 1200 UT on 15 December. This long-lasting positive storm effect is most apparent in ground-based GPS TEC and COSMIC TIP observations, while only a small increase in the topside ionosphere/plasmasphere TEC after 0400 UT is observed. This indicates that the long-lasting positive storm effect occurs predominantly at F region altitudes and, furthermore, that refilling of the topside ionosphere and plasmasphere is not the primary mechanism for producing the long-lasting positive storm phase during this event. The observations suggest that the enhanced eastward electric field and equatorward neutral wind are likely to play a significant role in the generation of long-lasting positive storm effects.

Citation: Pedatella, N. M., J. Lei, K. M. Larson, and J. M. Forbes (2009), Observations of the ionospheric response to the 15 December 2006 geomagnetic storm: Long-duration positive storm effect, *J. Geophys. Res.*, *114*, A12313, doi:10.1029/2009JA014568.

1. Introduction

[2] Energy injection at high latitudes that is associated with geomagnetic storms results in significant perturbations to the quiet time ionosphere. The corresponding global changes in the composition and dynamics of the ionosphere and thermosphere can produce both increases and decreases in electron densities and total electron content (TEC) [*Fuller-Rowell et al.*, 1994; *Prölss*, 1995; *Buonsanto*, 1999; *Mendillo*, 2006]. The observed increases and decreases in ionosphere F region electron densities and TEC are referred to as positive and negative storm effects, respectively. The occurrence and magnitude of the positive and negative storm effects is dependent upon the latitude, local time, and phase of the storm. Numerous observational and modeling studies have revealed the primary mechanisms that are thought to be responsible for these storm time effects (see reviews by *Prölss* [1995], *Buonsanto* [1999], *Mendillo* [2006], and *Burns et al.* [2007] and references therein). Despite these efforts, there remain gaps in the present understanding of how the ionosphere-thermosphere system responds to geomagnetic storms.

[3] It remains a grand challenge to understand the generation of long-lasting positive storm effects at low latitudes to midlatitudes [*Prölss*, 1995; *Burns et al.*, 2007] and several mechanisms have been proposed for producing the observed positive storm effects. One such mechanism is the downwelling of atomic oxygen at low latitudes to midlatitudes due to changes in thermospheric circulation [*Buonsanto*, 1999]. The downwelling of atomic oxygen results in an increase of atomic oxygen at F region altitudes and thus an increase in daytime F region electron densities and TEC. It has also been suggested that the observed

[1]Department of Aerospace Engineering Sciences, University of Colorado at Boulder, Boulder, Colorado, USA.

0148-0227/09/2009JA014568$09.00

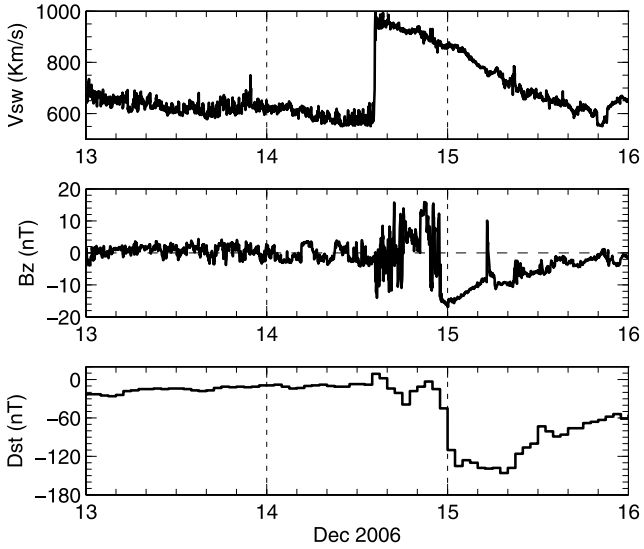

Figure 1. Solar wind speed, interplanetary magnetic field B_z, and D_{st} geomagnetic index on 13–15 December 2006.

positive storm effects are due to an enhancement in the equatorward neutral winds resulting from the high-latitude energy injection [*Prölss*, 1995]. The equatorward winds push the plasma up the magnetic field lines, resulting in an increase in the F layer height and subsequently a decrease in plasma loss rate and an increase in electron densities. In addition to equatorward winds, increased eastward electric fields can also lift up the ionosphere to altitudes where molecular recombination is less effective, and thus ionospheric F layer electron densities and TEC are enhanced and persist for a long duration [*Huang et al.*, 2005; *Lei et al.*, 2008a]. Another scenario that can explain long-lasting positive storm effects is due to the exchange of plasma between the ionosphere and plasmasphere. During geomagnetic storms, the outer plasmasphere is convected away due to enhanced magnetospheric electric fields and is refilled by ionospheric upflow [*Lemaire and Gringauz*, 1998; *Schunk and Nagy*, 2000]. The resulting vertical redistribution of plasma results in a decrease in the loss rate of electrons and thus a relative increase in electron densities and TEC compared with quiet time.

[4] The inability to separately observe electron densities in the F region ionosphere and the topside ionosphere/plasmasphere has made it difficult to assess the degree to which the refilling process contributes to the positive storm effect. While early studies made use of Faraday rotation observations to separate the integrated electron content into the ionospheric and plasmaspheric contribution [*Titheridge*, 1972; *Poletti-Liuzzi et al.*, 1977], these studies were limited in scope due to the limited spatial coverage of the observations. More recently, Global Positioning System (GPS) receivers onboard low-Earth orbiting (LEO) satellites have provided the opportunity to directly observe the topside ionosphere/plasmasphere TEC [*Mannucci et al.*, 2005; *Yizengaw et al.*, 2005, 2006]. Combined with ground-based GPS TEC observations, this approach offers good spatial coverage and the opportunity to separate the storm time response into an ionospheric contribution and the topside ionosphere/plasmasphere component. *Yizengaw et al.* [2005] illustrated the effectiveness of this technique by demonstrating that an observed decrease in ground-based TEC following the October 2003 geomagnetic storm was associated with a strong depletion in plasmaspheric electron densities.

[5] In the present paper we investigate the positive storm effect during the December 2006 geomagnetic storm using ground-based GPS TEC, TOPEX and Jason-1 TEC, and Constellation Observing System for Meteorology, Ionosphere, and Climate (COSMIC) topside ionosphere/plasmasphere TEC, GPS radio occultation electron density profiles and tiny ionospheric photometer (TIP) observations. This comprehensive set of observations allows for the exploration of the ionospheric response to the main and recovery phases of the December 2006 geomagnetic storm in different altitude regions. Using this unique set of observations, we are able to demonstrate the significance that uplifting of the F layer represents for producing the positive storm effect at low latitudes to midlatitudes. Furthermore, we make use of the topside ionosphere/plasmasphere TEC observations in order to determine the importance of plasmasphere refilling in producing long-lasting positive storm effects.

2. December 2006 Geomagnetic Storm

[6] A coronal mass ejection occurred on 13 December 2006 and produced an intense geomagnetic storm. Changes in the solar wind speed, interplanetary magnetic field (IMF) B_z, and the D_{st} index during this event are presented in Figure 1. The solar wind and IMF measurements are from the WIND satellite and are offset to account for the propagation time from the satellite location to the magnetopause. We have used WIND data due to the presence of data gaps in ACE observations of the solar wind parameters during this time period. A sudden increase in the solar wind speed occurred around 1400 universal time (UT) (shifted time) on 14 December, indicating the arrival of a shock. The storm sudden commencement (SSC) occurred at 1414 UT on 14 December (http://www.ngdc.noaa.gov/stp/SOLAR/ftpSSC.html). Following the initial shock, the solar wind speed gradually decayed. Following the SSC, the B_z component of the IMF oscillated rapidly for several hours, then turned northward for several hours, and finally turned southward around 2300 UT on 14 December. The D_{st} index rapidly decreased following the southward turning of the IMF B_z and reached a minimum value of −147 nT at 0800 UT on 15 December.

[7] A detailed analysis of the ionospheric response using a combination of observations and numerical modeling during the geomagnetic storm initial phase (1414 UT to 2300 UT on 14 December) is provided by *Lei et al.* [2008a]. The present paper focuses on the ionospheric positive storm effect on 15 December after the IMF B_z became southward at 2300 UT on 14 December.

3. Data Sources

3.1. Ground-Based Global Positioning System Total Electron Content

[8] Since the ionosphere represents a dispersive medium, dual-frequency GPS measurements from ground-based receivers can provide measurements of the TEC from the

Table 1. Orbital Altitude for COSMIC Satellites 1, 3, and 4 on 14 December at Different Points Along the Ascending and Descending Parts of the Orbit[a]

	COSMIC 1		COSMIC 3		COSMIC 4	
Latitude (°N)	Asc	Des	Asc	Des	Asc	Des
+60	505	515	513	525	515	525
0	510	530	510	535	510	538
−60	560	565	550	560	550	560

[a]Altitudes are in km. Asc, ascending; Des, descending.

surface of the Earth up to the GPS orbital altitude of approximately 20200 km [*Klobuchar*, 1996]. The GPS TEC is primarily dominated by electron densities in the F region ionosphere. TEC observations are a useful means for determining the effect of geomagnetic storms on the ionospheric plasma densities [*Mendillo*, 2006]. We use GPS TEC data obtained from the MIT Haystack Observatory Madrigal database (http://www.openmadrigal.org). A detailed description of the processing methods used to obtain the observations of ground-based GPS TEC is given by *Rideout and Coster* [2006].

3.2. TOPEX/Jason-1 Total Electron Content

[9] The TOPEX and Jason-1 satellites are in 1336 km altitude circular orbits and are equipped with dual-frequency radar altimeters in order to accurately measure sea surface height. The altimeters operate at 5.3 and 13.6 GHz and measurements on both frequencies can be used to estimate the TEC from the satellite to the surface of the ocean, which is then used to correct for the ionospheric delay [*Imel*, 1994]. The TOPEX and Jason-1 TEC data available through the NASA Physical Oceanography Distributed Active Archive Center (http://podaac.jpl.nasa.gov) are used in the present study.

3.3. COSMIC Observations

[10] The COSMIC consists of six microsatellites. They were launched in April 2006 with the goal of improving global weather prediction and space weather monitoring. The six satellites were initially placed into ∼500 km altitude orbits and over the 16 months following launch were raised to the final orbit altitude of ∼800 km. For the present study we have used observations from COSMIC-1, COSMIC-3,

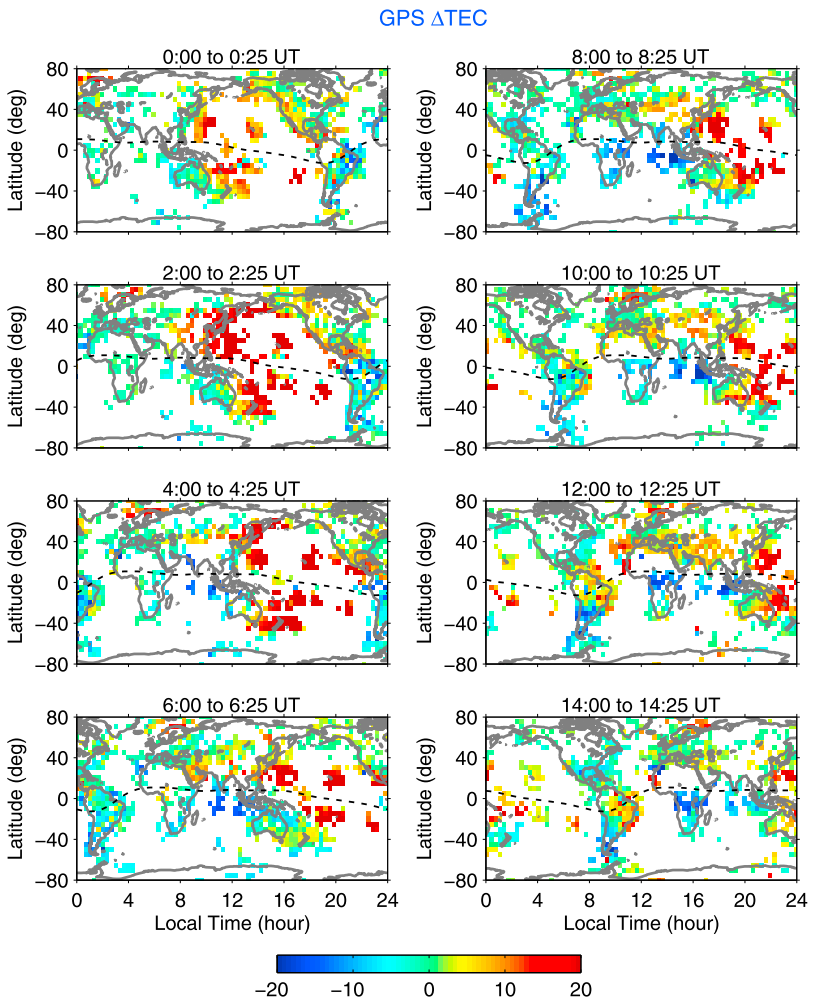

Figure 2. Differential ground-based GPS TEC from 0000–1400 UT between the storm day on 15 December and the undisturbed state on 13 December. The unit of differential TEC is TECu (1 TECu = 10^{16} electrons/m^2). The maximum TEC enhancements exceed 30 TECU during this period, while the color code is saturated at 20 TECU in order to better visualize the positive storm over the Pacific Ocean region. The geomagnetic equator is indicated by the dotted lines.

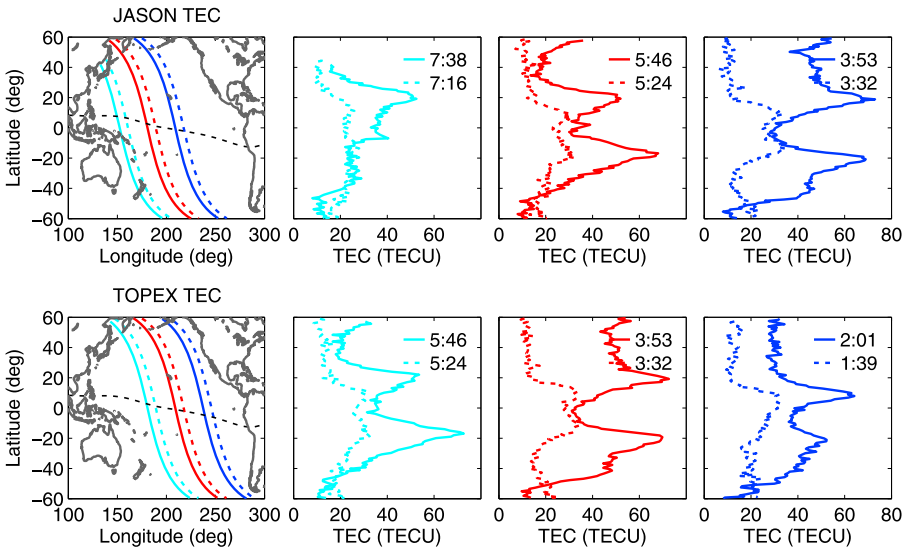

Figure 3. (top) Jason and (bottom) TOPEX TEC observations on 14 December (dashed) and 15 December (solid). The locations of the observations are shown in the maps on the left. The UT of the equatorial crossing for each pass is as indicated in the TEC plots. The local time of the observations was around 17.8 h.

and COSMIC-4. Due to orbit variations, the orbital altitude changes throughout the orbit and the altitude at different locations along the orbit for COSMIC-1, COSMIC-3, and COSMIC-4 during December 2006 are provided in Table 1. On 14 and 15 December, the local time of equatorial crossing for the three COSMIC satellites was near noon and midnight for the descending and ascending portions of the orbit, respectively. In order to meet the mission objectives, each satellite is equipped with two GPS antennae for radio occultation, two quasi-zenith GPS antennae for precise orbit determination (POD), a TIP, and a triband beacon (TBB) [*Rocken et al.*, 2000; *Cheng et al.*, 2006]. To obtain a comprehensive understanding of the storm effect on the ionosphere, we have used a combination of topside ionosphere/plasmasphere TEC measurements based on the POD data, electron density profiles using GPS radio occultation, and TIP observations. A detailed description of each of these observations is provided below.

[11] The quasi-zenith pointing GPS POD antennae are used to determine the TEC in the region between the COSMIC satellite and the 20200 km GPS orbital altitude. Since the COSMIC satellites are above the F region peak, this provides a measurement of the TEC in the topside ionosphere and plasmasphere. The relative line-of-sight TEC is derived from the dual-frequency GPS observations using standard techniques of leveling the carrier phase observations to the pseudorange observations [e.g., *Klobuchar*, 1996; *Mannucci et al.*, 1998, 1999]. Significant multipath due to signal reflections off of the solar panels on the COSMIC satellites can produce greater than 20 TEC unit (TECU) oscillations in the line-of-sight pseudorange TEC. In leveling the ambiguous carrier phase TEC to the absolute pseudorange TEC, the observations are weighted based on the observed multipath. This is done to minimize any errors that multipath may introduce. Recovering absolute line-of-sight TEC also requires that we account for the receiver and transmitter differential code biases (DCBs) which arise due to instrumental biases that are frequency dependent and are different for each receiver and transmitter [*Coco et al.*, 1991]. The GPS satellite biases estimated by the Center for Orbit Determination in Europe (CODE) [*Hugentobler et al.*, 2004] are used and the COSMIC satellite DCBs are estimated using high-latitude, nighttime observations [*Heise et al.*, 2002]. A geometric mapping function is used to convert the line-of-sight TEC observations above an elevation angle of 30° to obtain vertical TEC (VTEC) [*Klobuchar*, 1996]. In the event that multiple GPS satellites are above 30° elevation angle, the VTEC observations based on the line-of-sight TEC to each GPS satellite are averaged to obtain a single VTEC value at each epoch.

[12] In addition to measurements of the topside ionosphere/plasmasphere TEC, we make use of electron density profiles obtained through the technique of GPS radio occultation. *Schreiner et al.* [1999] and *Lei et al.* [2007] provide details on the use of GPS radio occultation to obtain electron density profiles. The derived electron density profiles are generally in good agreement with ionosonde and incoherent scatter radar profiles of electron density [*Lei et al.*, 2007]. In the present analysis we use electron density profiles obtained through the COSMIC Data Analysis and Archive Center (http://cosmic-io.cosmic.ucar.edu/cdaac/index.html).

[13] The TIP is a far ultraviolet radiometer that is used to observe the nighttime ionospheric airglow OI 135.6 nm emission. The OI 135.6 nm emission is primarily due to the radiative recombination of O^+ ions and is related to the electron density. Since the TIP is directed in the nadir direction, the TIP observations are related to the vertical TEC below the COSMIC satellites and also the F layer maximum electron density [*Dymond et al.*, 2000; *Wu et al.*, 2005].

4. Observations

4.1. Ground-Based GPS and TOPEX/Jason-1 Observations of Long-Lasting Positive Storm Phase

[14] Global maps of the differential ground-based GPS TEC from 0000 to 1400 UT between 13 and 15 December

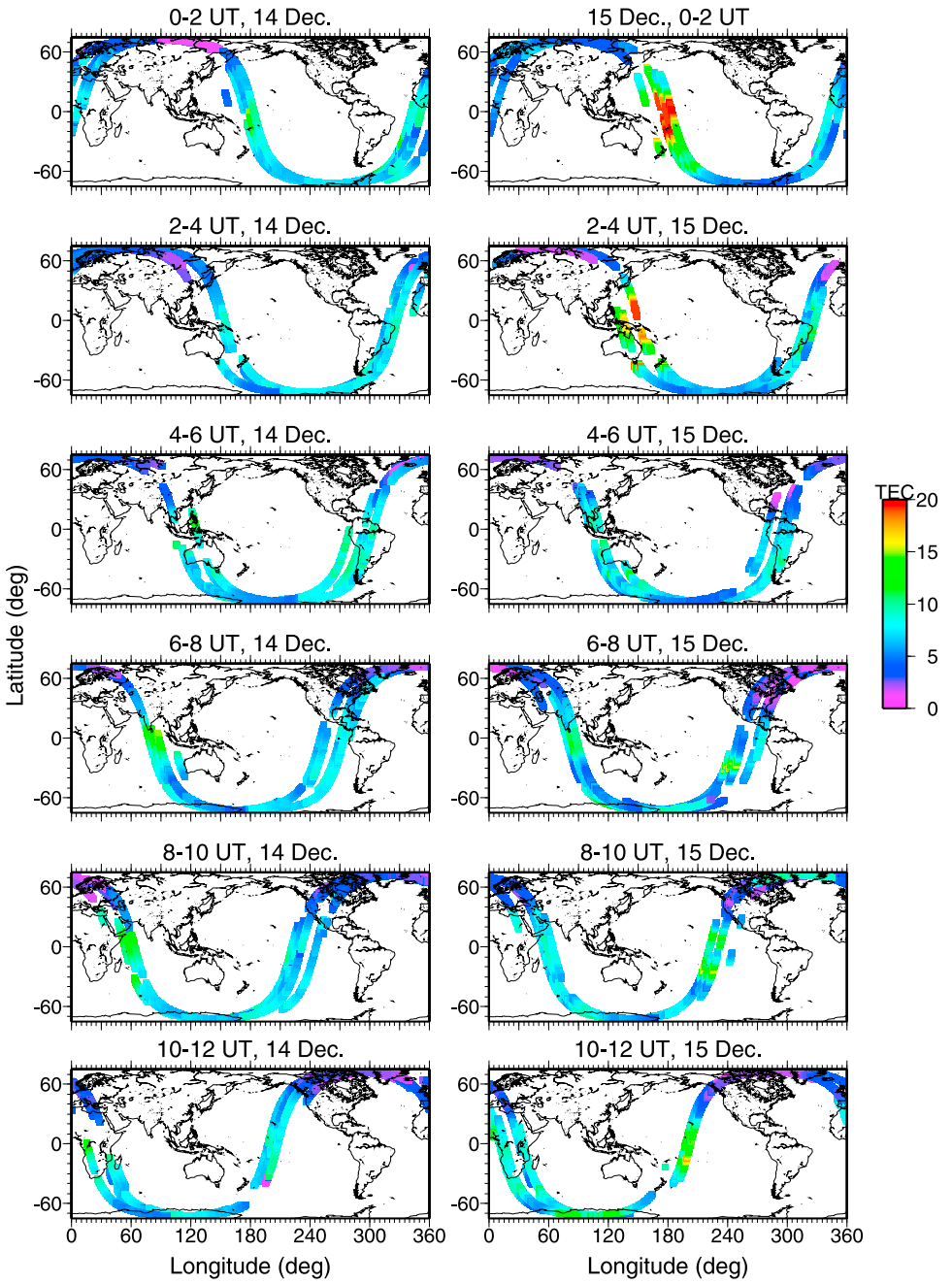

Figure 4. Global maps of the topside VTEC (in units of TECu; 1 TECu = 10^{16} electrons/m^2) based on observations from COSMIC 1, 3, and 4 between 0000–1400 UT on (left) 14 December and (right) 15 December.

are shown in Figure 2. Note that Figure 2 is latitude versus local time and the world map shifts as the UT changes. Both positive and negative storm effects can be seen at low latitudes to midlatitudes beginning at 0000 UT on 15 December. As the present study is focused on determining the mechanisms responsible for generating positive storm effects, we will limit our discussion to the observations of storm time enhancements in TEC. Enhancements in excess of 20 TECU with respect to the quiet time values are observed at low latitudes to midlatitudes over the Pacific Ocean beginning around 0200 UT indicating a large positive storm effect. The observed positive storm effect appears to extend from the equator to around 60° N geographic latitude. However, the lack of ground-based GPS TEC observations at high latitudes makes it difficult to completely assess the latitudinal extent of the positive storm effect. At 0200 UT the Pacific Ocean region is in early afternoon to evening local times. The large positive storm effect over this region remains present until 1200 UT with smaller enhancements remaining at low latitudes until 1400 UT. By this time the Pacific Ocean region has rotated into the nighttime sector. This reveals that the enhancements in ground-based TEC over the Pacific Ocean on 15 December lasted for more than 12 h, and it can thus be considered a long-lasting positive storm effect.

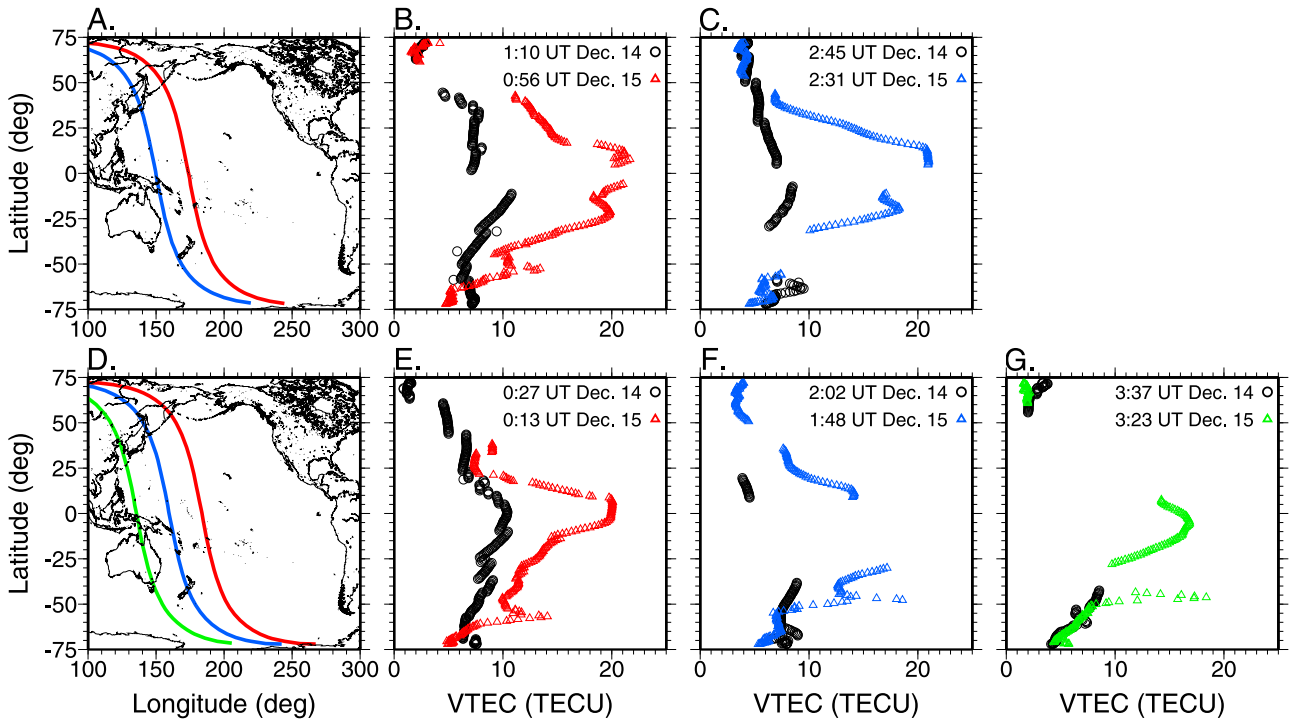

Figure 5. (a) Ground track of COSMIC 1 for two passes over the Pacific Ocean on 14 and 15 December. (b and c) COSMIC 1 VTEC observations on 14 and 15 December for the two passes shown in Figure 5a. (d) Ground track of COSMIC 4 for three passes over the Pacific Ocean on 14 and 15 December. (e–g) COSMIC 4 VTEC observations on 14 and 15 December for the three passes shown in Figure 5d. The equator crossing time for each pass is indicated.

[15] Due to the relative sparsity of ground-based GPS TEC observations over the Pacific Ocean, we have used TOPEX and Jason-1 TEC observations to reveal the latitudinal extent and structure of the positive storm phase in greater detail. TOPEX and Jason-1 TEC observations on 14 and 15 December are shown in Figure 3. The local time of the equatorial crossing was around 17.8 h for the TOPEX and Jason-1 passes shown in Figure 3. The observations on 14 December occurred prior to the SSC and are representative of the undisturbed ionosphere. We have used 14 December instead of 13 December as representative of the quiet time ionosphere to minimize the longitudinal difference between the quiet time and storm time observations. Similar to the ground-based GPS TEC observations, the TOPEX/Jason-1 TEC reveal a significant positive storm phase over the Pacific Ocean beginning around 0200 UT and lasting for several hours. The largest enhancements are in excess of 30 TECU and occur at the equatorial ionization anomaly (EIA) crest regions. The large increases in crest region densities along with the more structured EIA on 15 December demonstrate that an enhancement in the EIA strength occurred during this time period. Enhancements in equatorward neutral winds may also be responsible for the large TEC enhancements at low latitudes. The TOPEX/Jason-1 TEC observations also reveal a hemispherical asymmetry with the increases in TEC extending to higher latitudes in the northern hemisphere. The observations at 0400 UT show large enhancements at 60° N geographic latitude and this leads us to believe that the positive storm effects may have reached latitudes poleward of 70° N.

4.2. COSMIC Observations

[16] Global maps of the topside ionosphere/plasmasphere TEC based on observations from COSMIC-1, COSMIC-3, and COSMIC-4 from 0000-1200 UT on 14 and 15 December are shown in Figure 4. The observations on 14 December are representative of the quiet time ionosphere as this was prior to the SSC at 1414 UT. The data gaps are due to either missing GPS observations, poor data quality or no GPS satellites being above 30° elevation angle. The storm time enhancement of plasma densities observed in the ground-based GPS TEC and TOPEX/Jason-1 TEC over the Pacific Ocean is also clearly seen in the COSMIC topside ionosphere/plasmasphere TEC during 0000–0400 UT on 15 December. Although the enhancements are greatest at low latitudes, increases in the topside ionosphere/plasmasphere TEC are observed in the northern hemisphere at all latitudes covered by the COSMIC satellites. In the southern hemisphere, positive storm effects are observed equatorward of around −60° N geographic latitude and the topside ionosphere/plasmasphere TEC decreases poleward of this latitude. Although the enhancements are smaller, positive storm effects over the Pacific Ocean region are still seen in the topside ionosphere/plasmasphere TEC from 0800–1200 UT on 15 December when the COSMIC satellites again pass over this region.

[17] The topside ionosphere/plasmasphere TEC for two COSMIC-1 and three COSMIC-4 passes over the Pacific Ocean on 14 and 15 December are shown in Figure 5 in order to more clearly illustrate the storm time effects. The equatorial crossing time for these passes was near noon. The

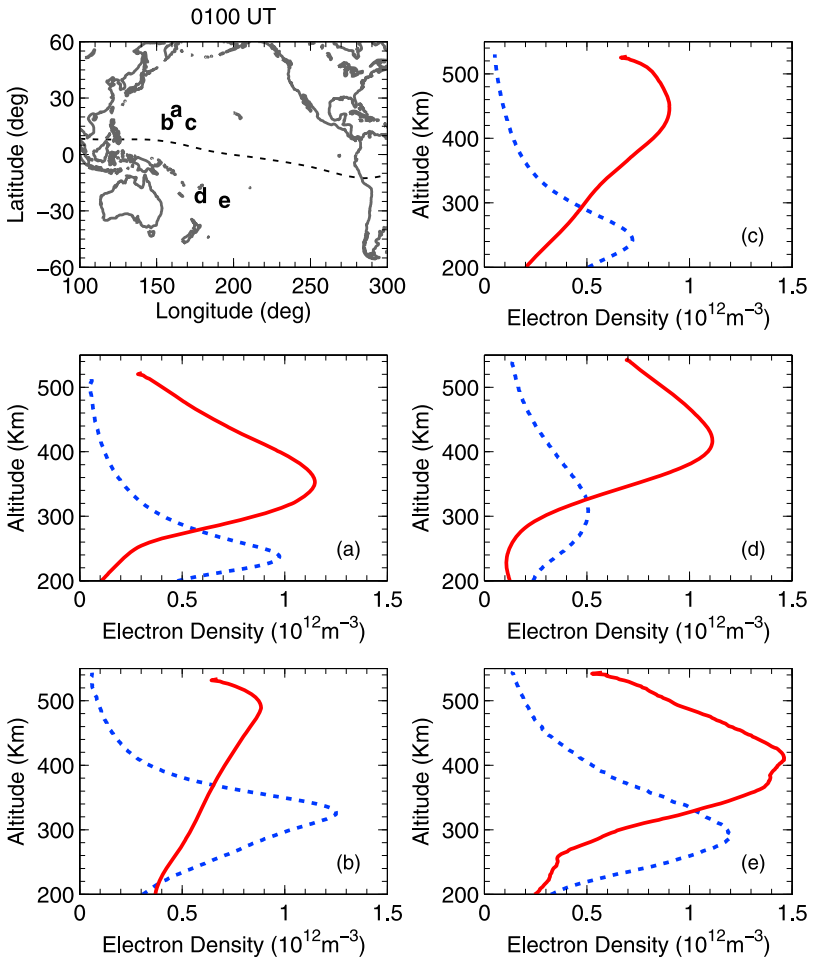

Figure 6. Comparison of vertical electron density profiles based on COSMIC radio occultation on 14 December (dashed blue) and 15 December (solid red). The locations of the electron density profiles are indicated in the map at the top left.

small 1–2 TECU "jumps" in the data occur when a GPS satellite either goes above or below the 30° elevation angle cutoff and are due to averaging observations of TEC from multiple GPS satellites. However, the 1–2 TECU changes are considered to be small enough that they do not impact the present analysis. Some large data gaps are present and these are due to the reasons discussed previously. As can be seen in Figure 5, the topside ionosphere/plasmasphere TEC exhibits enhancements greater than 10 TECU on 15 December. The largest enhancements are at low latitudes and the COSMIC-1 observations (Figures 5a–5c) demonstrate increases as large as 15 TECU in the EIA crest regions. A narrow region of significantly increased topside ionosphere/plasmasphere TEC is also observed near −50° N geographic latitude and this may be associated with the effects of soft particle precipitation.

[18] Electron density profiles from COSMIC GPS radio occultations on 14 and 15 December are shown in Figure 6. All of the electron density profiles shown occurred near 0100 UT when this region was around noon local time. The electron density profiles clearly reveal that the F layer peak height increased by over 100 km at low latitudes in both hemispheres. Increases in electron density at the F layer peak height are also observed at all locations except for the electron density profile at location b, which is closer to the geomagnetic equator. It is worth noting that significant spatial variability is observed in the maximum electron density values on 14 December and that less variability is present during the geomagnetic storm on 15 December. For example, the maximum electron density in profiles b and c is nearly the same on 15 December, whereas on 14 December the maximum electron density for profile b is almost twice that of profile c. This indicates that strong storm time effects may mask the spatial variations observed in the maximum electron density values during quiet time, and it is also related to the redistribution of density in the topside ionosphere during the storm.

[19] Observations from the TIP onboard COSMIC-1 for four passes over the Pacific Ocean are shown in Figure 7. The TIP observations from COSMIC-3 and COSMIC-4 show similar results to COSMIC-1 and have thus been omitted. The TIP observations shown in Figure 7 occurred near midnight local time. Storm time enhancements in the TIP count, and hence F region electron densities and TEC below COSMIC-1, are observed at all latitudes covered by the TIP observations. The largest enhancements are observed to occur in the EIA crest regions. A slight hemispheric asymmetry exists with the enhancements being

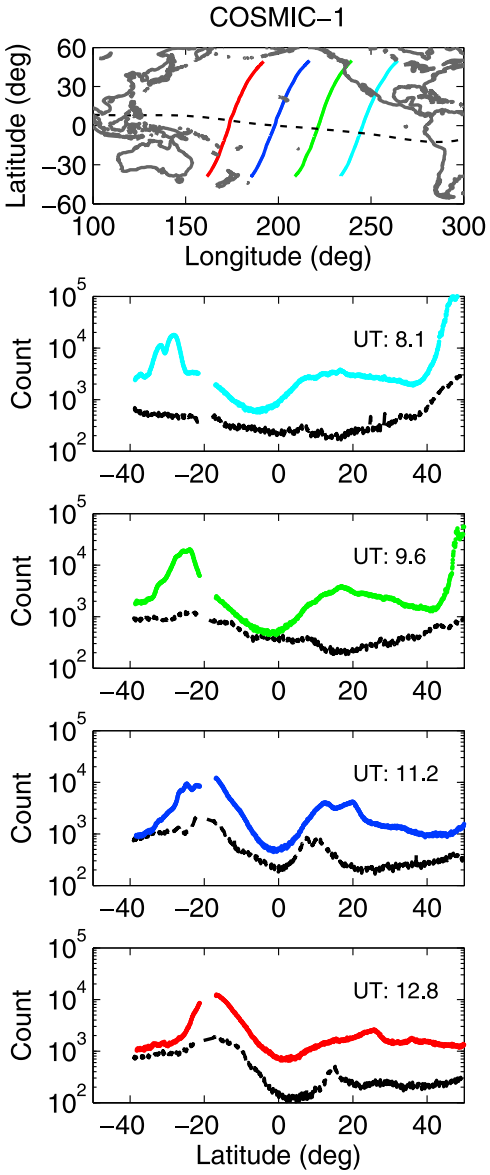

Figure 7. (top) Ground track of COSMIC 1 for four passes over the Pacific Ocean on 15 December. (bottom) Raw TIP counts for each of the four passes shown in Figure 7 (top) along with the quiet time observations from 14 December (black). The UT of each pass is indicated. The equator crossing local time was near midnight for each of the passes shown.

both larger and occurring at higher latitudes in the southern hemisphere. Significant enhancements in the TIP count are also observed poleward of 40° N geographic latitude for the first two passes.

5. Discussion

[20] We now turn our attention to the discussion of the observations presented in section 4 and address the primary mechanisms that are thought to be responsible for producing the prolonged positive storm effect on 15 December. During the initial hours of the storm main phase (0000–0400 UT on 15 December) large enhancements are observed in the ground-based GPS TEC, TOPEX/Jason-1 TEC, and the topside ionosphere/plasmasphere TEC at latitudes equatorward of ~60° over the Pacific Ocean region. Although the positive storm effects extend to midlatitudes, the largest enhancements are concentrated near the EIA crests. The TOPEX/Jason-1 TEC observations (Figure 3) during this time period show a significant enhancement in the EIA strength, and this suggests storm time changes in the low-latitude electric fields and equatorial vertical drift velocity [e.g., *Fejer*, 1997]. It is, however, interesting to note that small positive storm effects are also observed over the equatorial region during this time period. The storm time enhancement in the EIA trough region is likely due to the effect of equatorward neutral winds in the thermosphere [*Lin et al.*, 2005; *Balan et al.*, 2009]. The influence that equatorward neutral winds and changes in the low-latitude electric fields have on the generation of the positive storm effect will be disucussed in more detail later.

[21] The COSMIC electron density profiles in Figure 6 show that the F layer peak height was increased by greater than 100 km over the Pacific Ocean region around 0100 UT (early afternoon local time) on 15 December. This uplifting of the F layer is also thought to produce the enhancements in topside ionosphere/plasmasphere TEC that can be as large as 50% (greater than 14 TECU) of the ground-based GPS TEC in the equatorial region. Uplifting of the F layer will result in greater electron densities above the altitude of the COSMIC satellites, producing the large enhancements in topside ionosphere/plasmasphere TEC that we have observed. Using the Coupled Magnetosphere Ionosphere Thermosphere (CMIT) model, *Lei et al.* [2008b] showed that both TADs and increased vertical drifts occurred at low latitudes to midlatitudes over eastern Asia during 0000–0400 UT on 15 December. Their modeling results are consistent with the COSMIC observations, which demonstrate that enhanced equatorward neutral winds and upward drifts are responsible for producing the large positive storm effects observed at the crest regions in both hemispheres by ground-based GPS TEC and TOPEX/Jason-1 TEC over the Pacific Ocean region. It should be pointed out that the CMIT simulations were able to reproduce ionosonde observations and TIDs on 15 December over Japan as shown by *Lei et al.* [2008b] and capture the positive storm effect at the EIA crest regions during 0000–0300 UT; however, the model was unable to reproduce the long-lasting positive effects that we have observed. The CMIT simulation also showed a depletion in plasma densities over the equatorial region between 0000 and 0300 UT on 15 December which is not consistent with the observations and will be discussed later.

[22] A large positive storm also occurred in the daytime during the initial phase of the December 2006 geomagnetic storm [*Lei et al.*, 2008a]. Although there is similarity in the structure of the positive storm effects during the initial phase on 14 December and during the main phase on 15 December, the positive storm effects on 15 December persisted more that 12 h and were observed beyond midnight. Additionally, the processes responsible for the positive storm effects should be different. During the initial phase, the IMF B_z oscillated rapidly and changes in the electric fields played a major role in producing the daytime positive storm. Different geophysical conditions existed

during the storm main phase and B_z was southward for an extended time period. This results in the thermosphere and ionosphere being disturbed for a longer time period.

[23] One interesting feature of the ionospheric storm time response that was only observed by the COSMIC observations of topside ionosphere/plasmasphere TEC are the ~10 TECU increases that occurred near −50° N geographic latitude. We believe these enhancements are due to soft particle precipitation associated with an equatorward movement of the poleward boundary of the trough region [*Prölss et al.*, 1991]. It is interesting to note that this spike is very weak in the TOPEX/Jason-1 TEC observations. This indicates that the effects of soft particle precipitation are more significant for electron densities in the topside ionosphere and do not significantly impact electron densities near the F region peak. The reason for this difference is currently unknown. However, it may be related to fast diffusion in the upper F region and large recombination rate at lower altitudes; or, it may be due to an increase in the topside ionosphere scale height due to energetic particles heating the plasma which will result in an increase in the topside ionosphere/plasmasphere TEC.

[24] Both the COSMIC TIP and ground-based GPS TEC observations reveal that the large positive storm effect in the EIA crest regions over the Pacific Ocean remained present until beyond 1200 UT on 15 December. A potential source of this long-lasting positive storm effect is the refilling of the topside ionosphere and plasmasphere. During 1000–1400 UT on 15 December, the topside ionosphere/plasmasphere TEC has only increased by a few TECU compared to the quiet time values as demonstrated by the COSMIC observations in Figure 4. This small increase in the topside ionosphere/plasmasphere TEC leads us to believe that the enhancements in ground-based GPS TEC during this time over the Pacific Ocean are primarily due to changes in F region electron densities. We can thus conclude that the ionospheric upflow to refill the topside ionosphere/plasmasphere is not the primary mechanism for producing the long-lasting positive storm effect that was observed by the ground-based GPS TEC on 15 December. It was previously thought that the failure of the CMIT simulation to reproduce the long-lasting positive storm effect over the Pacific Ocean region was due to the fact that the CMIT model has an upper boundary of about 500–600 km in this event for the ionosphere/thermosphere domain and thus is not able to simulate the effects of ionosphere/plasmasphere coupling. However, the COSMIC observations of topside ionosphere/plasmasphere TEC indicate that the lack of a plasmasphere module in the CMIT model is not the primary reason why the model simulation does not produce a long-lasting positive storm phase.

[25] As the refilling of the topside ionosphere/plasmasphere does not appear to be responsible for the long-lasting positive storm effect, the question remains as to why the positive storm effects persisted from local evening to postmidnight (in excess of 12 h) over the Pacific Ocean region. *Yue* [2008] performed a numerical simulation using a 40 m/s vertical drift velocity with only a 2 h duration in the flux tube ionospheric model under solar minimum conditions. The simulation results showed that the TEC increases by about 30 TECU in the EIA crest regions and decays to 10 TECU after about 12 h, while the equatorial region shows a strong depletion. The persistence of the positive storm at the EIA crest regions is consistent with the observations we have presented. However, the observations showed a weak positive storm in the equatorial region (Figures 2, 3, and 7), which is in contrast to the depletions modeled by both *Yue* [2008] and the CMIT simulation. Modeling results by *Lin et al.* [2005] and *Balan et al.* [2009] showed that an equatorward neutral wind can enhance the positive storm effects at both the EIA crest and equatorial regions. Therefore, our observations suggest that the equatorward neutral wind likely plays an important role in producing the positive storm effect in the equatorial region, and in maintaining the positive storm effect produced by the eastward electric fields during 0000–0400 UT on 15 December as shown by *Lei et al.* [2008b]. Neutral composition changes could also produce the long-lasting positive storm effect; however, analysis of TIMED/GUVI O/N_2 ratio observations do not reveal any enhancement in the equatorial region on 15 December. In addition, equatorial vertical drifts after sunset associated with disturbance dynamo electric fields [*Blanc and Richmond*, 1980] may play a role in maintaining the positive storm effects. If this is the case, however, the disturbance neutral winds would reduce the eastward electric field and weaken the positive storm during the daytime. The failure in simulating the positive storm in the equatorial region by the CMIT indicates that the neutral wind pattern may not be simulated well over the Pacific Ocean region during this event. In addition, the short duration of the positive storm from the CMIT simulation may be due to the same reasons put forth by *Burns et al.* [2008] to explain why the ionospheric density quickly decays after dusk in the thermosphere-ionosphere-electrodynamics general circulation model (TIEGCM). However, these hypotheses cannot be tested without direct observations of the thermosphere.

6. Conclusions

[26] Through the use of observations from ground-based GPS receivers and the TOPEX, Jason-1, and COSMIC satellites, we have explored the long-duration ionospheric positive storm effect that occurred on 15 December 2006. Such a combination of observations has provided a unique view of the ionospheric storm time response and provides the opportunity to explore the response in different altitude regions. Based on these observations we have reached the following conclusions:

[27] 1. A significant enhancement of plasma densities in the EIA crest region and the topside ionosphere/plasmasphere TEC over the equatorial region was observed during the initial hours of the December 2006 storm main phase. Moreover, the positive storm effects in the EIA crest regions remained present for more than 12 h.

[28] 2. Soft particle precipitation resulted in significant enhancements in the topside ionosphere/plasmasphere TEC near −50° N geographic latitude. This effect was observed above ~550 km leading us to believe that the soft particle precipitation primarily influences electron densities in the topside ionosphere and plasmasphere. The TOPEX/Jason-1 observations measure TEC below around 1300 km and should also display the effects of the soft particle precipitation. However, this effect is less significant in the TOPEX/

Jason-1 TEC indicating that processes in the F region overshadow the soft particle precipitation effect.

[29] 3. Long-lasting positive storm effects were observed in the EIA crest regions, however, these effects were significantly smaller in the topside ionosphere/plasmasphere TEC after 0300 UT on 15 December. This indicates that refilling of the topside ionosphere and plasmasphere is not responsible for producing these long-lasting effects. Rather, a combination of eastward electric fields and equatorward neutral winds may produce the observed positive ionospheric storm, and the equatorward neutral winds may also be an important driver for maintaining the positive storm effect to persist for more that 12 h.

[30] **Acknowledgments.** The authors wish to thank the providers of data used in the present study. We thank W. Wang and A. G. Burns for helpful discussions and also B. Zhao and S. Syndergaard for their assistance in processing the TOPEX/Jason-1 and COSMIC data. This work was supported by NASA grant NNX09AI11G and NSF EAR 0538116 to the University of Colorado.

[31] Wolfgang Baumjohann thanks I. Kutiev and another reviewer for their assistance in evaluating this paper.

References

Balan, N., K. Shiokawa, Y. Otsuka, S. Watanabe, and G. J. Bailey (2009), Super plasma fountain and equatorial ionization anomaly during penetration electric field, *J. Geophys. Res.*, *114*, A03310, doi:10.1029/2008JA013768.

Blanc, M., and A. D. Richmond (1980), The ionospheric disturbance dynamo, *J. Geophys. Res.*, *85*, 1669–1680.

Buonsanto, M. J. (1999), Ionospheric storms—A review, *Space Sci. Rev.*, *88*, 563–601.

Burns, A. G., S. C. Solomon, W. Wang, and T. L. Killeen (2007), The ionospheric and thermospheric response to CMEs: Challenges and successes, *J. Atmos. Sol. Terr. Phys.*, *69*, 77–85.

Burns, A. G., W. Wang, M. Wiltberger, S. C. Solomon, H. Spence, T. L. Killeen, R. E. Lopez, and J. E. Landivar (2008), An event study to provide validation of TING and CMIT geomagnetic middle-latitude electron densities at the F_2 peak, *J. Geophys. Res.*, *113*, A05310, doi:10.1029/2007JA012931.

Cheng, C.-Z. F., Y.-H. Kuo, R. A. Anthes, and L. Wu (2006), Satellite constellation monitors global and space weather, *Eos Trans. AGU*, *87*(17), 166.

Coco, D. S., C. Coker, S. R. Dahlke, and J. R. Clynch (1991), Variability of GPS satellite differential group delay biases, *IEEE Trans. Aerosp. Electron. Syst.*, *27*, 931–938.

Dymond, K. F., J. B. Nee, and R. J. Thomas (2000), The tiny ionospheric photometer: An instrument for measuring ionospheric gradients for the COSMIC constellation, *Terr. Atmos. Ocean Sci.*, *11*, 273–290.

Fejer, B. G. (1997), The electrodynamics of the low-latitude ionosphere: Recent results and future challenges, *J. Atmos. Sol. Terr. Phys.*, *59*(13), 1465–1482.

Fuller-Rowell, T. J., M. V. Codrescu, R. J. Moffett, and S. Quegan (1994), Response of the thermosphere and ionosphere to geomagnetic storms, *J. Geophys. Res.*, *99*, 3893–3914.

Heise, S., N. Jakowski, A. Wehrenpfennig, Ch. Reigber, and H. Lühr (2002), Sounding of the topside ionosphere/plasmasphere based on GPS measurements from CHAMP: Initial results, *Geophys. Res. Lett.*, *29*(14), 1699, doi:10.1029/2002GL014738.

Huang, C.-S., J. C. Foster, L. P. Goncharenko, P. J. Erickson, W. Rideout, and A. J. Coster (2005), A strong positive phase of ionospheric storms observed by the Millstone Hill incoherent scatter radar and global GPS network, *J. Geophys. Res.*, *110*, A06303, doi:10.1029/2004JA010865.

Hugentobler, U., et al. (2004), CODE IGS Analysis Center Technical Report 2002, in *IGS 2001–2002 Technical Reports*, edited by K. Gowey, R. Neilan, and A. Moore, IGS Cent. Bur., Jet Propul. Lab., Pasadena, Calif.

Imel, D. (1994), Evaluation of the TOPEX/POSEIDON dual-frequency ionosphere correction, *J. Geophys. Res.*, *99*(C12), 24,895–24,906.

Klobuchar, J. A. (1996), Ionospheric effects on GPS, in *Global Positioning System: Theory and Applications*, vol. I, edited by B. W. Parkinson and J. J. Spilker, pp. 485–515, Am. Inst. of Aeronaut. and Astronaut, New York.

Lei, J., et al. (2007), Comparison of COSMIC ionospheric measurements with ground-based observations and model predictions: Preliminary results, *J. Geophys. Res.*, *112*, A07308, doi:10.1029/2006JA012240.

Lei, J., W. Wang, A. G. Burns, S. C. Solomon, A. D. Richmond, M. Wiltberger, L. P. Goncharenko, A. Coster, and B. W. Reinisch (2008a), Observations and simulations of the ionospheric and thermospheric response to the December 2006 geomagnetic storm: Initial phase, *J. Geophys. Res.*, *113*, A01314, doi:10.1029/2007JA012807.

Lei, J., A. G. Burns, T. Tsugawa, W. Wang, S. C. Solomon, and M. Wiltberger (2008b), Observations and simulations of quasiperiodic ionosphere oscillations and large-scale traveling ionospheric disturbances during the December 2006 geomagnetic storm, *J. Geophys. Res.*, *113*, A06310, doi:10.1029/2008JA013090.

Lemaire, J. F., and K. I. Gringauz (1998), *The Earth's Plasmasphere*, Cambridge Univ. Press, New York.

Lin, C. H., A. D. Richmond, R. A. Heelis, G. J. Bailey, G. Lu, J. Y. Liu, H. C. Yeh, and S.-Y. Su (2005), Theoretical study of the low- and mid-latitude ionospheric electron density enhancement during the October 2003 superstorm: Relative importance of the neutral wind and the electric field, *J. Geophys. Res.*, *110*, A12312, doi:10.1029/2005JA011304.

Mannucci, A., B. D. Wolson, D. N. Yuan, C. H. Ho, U. J. Lindqwister, and T. F. Runge (1998), A global mapping technique for GPS-derived ionospheric total electron content measurements, *Radio Sci.*, *33*(3), 565–582.

Mannucci, A., J. B. A. Iijima, U. J. Linqwister, X. Pi, L. Sparks, and B. D. Wilson (1999), GPS and ionosphere, in *Review of Radio Science 1996–1999*, edited by W. R. Stone, pp. 625–665, Int. Union of Radio Sci., Ghent, Belgium.

Mannucci, A. J., B. T. Tsurutani, B. A. Iijima, A. Komjathy, A. Saito, W. D. Gonzalez, F. L. Guarnieri, J. U. Kozyra, and R. Skoug (2005), Dayside global ionospheric response to the major interplanetary events of October 29–30, 2003 "Halloween Storms", *Geophys. Res. Lett.*, *32*, L12S02, doi:10.1029/2004GL021467.

Mendillo, M. (2006), Storms in the ionosphere: Patterns and processes for total electron content, *Rev. Geophys.*, *44*, RG4001, doi:10.1029/2005RG000193.

Poletti-Liuzzi, D. A., K. C. Yeg, and C. H. Liu (1977), Radio beacon studies of the plasmasphere, *J. Geophys. Res.*, *82*, 1106–1114.

Prölss, G. W. (1995), Ionospheric F-region storms, in *Handbook of Atmospheric Electrodynamics*, edited by H. Volland, CRC Press, Boca Raton, Fla.

Prölss, G. W., L. H. Brace, H. G. Mayr, G. R. Carignan, T. L. Killeen, and J. A. Klobuchar (1991), Ionospheric storm effects at subauroral latitudes: A case study, *J. Geophys. Res.*, *96*(A2), 1275–1288.

Rideout, W., and A. Coster (2006), Automated GPS processing for global total electron content data, *GPS Solutions*, *10*, 219–228, doi:10.1007/s10291-006-0029-5.

Rocken, C., Y.-H. Kuo, W. Schreiner, D. Hunt, S. Sokolovskiy, and C. McCormick (2000), COSMIC system description, *Terr. Atmos. Ocean Sci.*, *11*, 21–52.

Schreiner, W. S., S. V. Sokolovskiy, C. Rocken, and D. C. Hunt (1999), Analysis and validation of GPS/MET radio occultation data in the ionosphere, *Radio Sci.*, *34*(4), 949–966.

Schunk, R. W., and A. F. Nagy (2000), *Ionospheres: Physics, Plasma Physics, and Chemistry*, Cambridge Univ. Press, New York.

Titheridge, J. E. (1972), Determination of ionospheric electron content from Faraday rotation of geostationary satellite signals, *Planet. Space Sci.*, *20*, 353–369.

Wu, B., V. Chu, P. Chen, and T. Ting (2005), FORMOSAT-3/COSMIC science mission update, *GPS Solutions*, *9*, 111–121, doi:10.1007/S102910050140z.

Yizengaw, E., M. B. Moldwin, P. L. Dyson, and T. J. Immel (2005), Southern Hemisphere ionosphere and plasmasphere response to the interplanetary shock event of 29–31 October 2003, *J. Geophys. Res.*, *110*, A09S30, doi:10.1029/2004JA010920.

Yizengaw, E., M. B. Moldwin, A. Komjathy, and A. J. Mannucci (2006), Unusual topside ionospheric density response to the November 2003 superstorm, *J. Geophys. Res.*, *111*, A02308, doi:10.1029/2005JA011433.

Yue, X. (2008), Modeling and data assimilation of mid- and low-latitude ionosphere, Ph.D. thesis, 116 pp., Chin. Acad. of Sci., Beijing.

J. M. Forbes, K. M. Larson, J. Lei, and N. M. Pedatella, Department of Aerospace Engineering Sciences, University of Colorado at Boulder, 429 UCB, Boulder, CO 80309, USA. (forbes@colorado.edu; kristinem.larson@gmail.com; jiuhou.lei@colorado.edu; nicholas.pedatella@colorado.edu)